

Microstructural Evolution of Advanced Radiation-Resistant ODS Steel with Different Lengths of Mechanical Alloying Time

Sanghoon Noh*, Ga Eon Kim, Suk Hoon Kang, Tae Kyu Kim

Nuclear Materials Division, Korea Atomic Energy Research Institute, Yuseong-gu, Daejeon, Republic of Korea

*Corresponding author: shnoh@kaeri.re.kr

1. Introduction

Sodium cooled fast reactor (SFR) is considered to be one of the next generation nuclear systems with enhanced economics, stability, and reliability. For realization of this system, it is inevitable to develop the advanced structural material having both high strength and irradiation resistance at high temperatures [1]. Austenitic stainless steel may be one of the candidates because of good strength and corrosion resistance at the high temperatures, however irradiation swelling well occurred to 120dpa at high temperatures and this leads the decrease of the mechanical properties and dimensional stability [2]. Compared to this, ferritic/martensitic steel is a good solution because of excellent thermal conductivity and good swelling resistance. Unfortunately, the available temperature range of ferritic/martensitic steel is limited up to 650°C [3]. ODS steel is the most promising structural material because of excellent creep and irradiation resistance by uniformly distributed nano-oxide particles with a high density which is extremely stable at the high temperature in ferritic/martensitic matrix. Recently, advanced radiation-resistant ODS steel (ARROS) has been newly developed for the in-core structural components in SFR. The ARROS was designed in the basis of martensitic phase to have high homogeneity, productivity and reproducibility. In this study, effect on microstructures of the ARROS with different length of mechanical alloying time was investigated. Microstructural evolutions as well as powder properties were examined to determine the optimized condition of the fabrication process.

2. Methods and Results

2.1 Experimental procedure

The ARROS is Fe(bal.)-10Cr-1Mo (in wt.%) martensitic ODS steel. Pre-alloyed powder without Y_2O_3 was fabricated by a vacuum induction melting and Ar-gas atomization processes. The chemical composition of the pre-alloyed powder was summarized in Table 1. The ODS steel were fabricated by mechanical alloying (MA) and uniaxial hot pressing (UHP) processes. The MA is essential process that the continuous collision between grinding media and raw

powders with a high revolving energy makes the repeated crushes and cold welding of powders, which eventually create the homogenous mixing and alloying in the constitution elements. The pre-alloyed powders and Y_2O_3 powder were mechanically alloyed by a high energy horizontal ball-mill apparatus, Simoloyer CM-20. Mechanical alloying atmosphere was thoroughly controlled in ultra-high purity argon (99.9999%) gas. The mechanical alloying was performed with a ball-to-powder weight ratio of 10:1. To investigate the effects of the MA time, powders were mechanically alloyed for various times. After the MA process, powder properties such as surface morphology, particle size and crystalline phase were evaluated. Particle size distribution was measured using a laser diffraction scattering method with a particle size analyzer. SEM was utilized to observe the surface morphology. The crystalline phase of MA powders was evaluated by X-ray diffraction (XRD) analysis. The MA powder was then consolidated using UHP at 1150°C for 2h at a heating rate of 10°C/min. The process was carried out in a high vacuum ($<5 \times 10^{-4}$ Pa) under hydrostatic pressure of 80 MPa in uni-axial compressive loading mode. After the process, the hydrostatic pressure was relieved and the samples were cooled in the furnace. Normalizing and tempering heat treatments was also done at 1150°C for 60 min and at 750°C for 30 min, respectively. The microstructures were observed by electron microscopes.

Table 1: Chemical composition of pre-alloyed powder

Elements	Compositions, wt.%
Fe	bal.
C	0.082
Cr	10.03
Mo	0.99
Mn	0.50
Ti	0.08
V	0.17
O	0.015

2.2 Evolution of powder properties with different length of mechanical alloying time

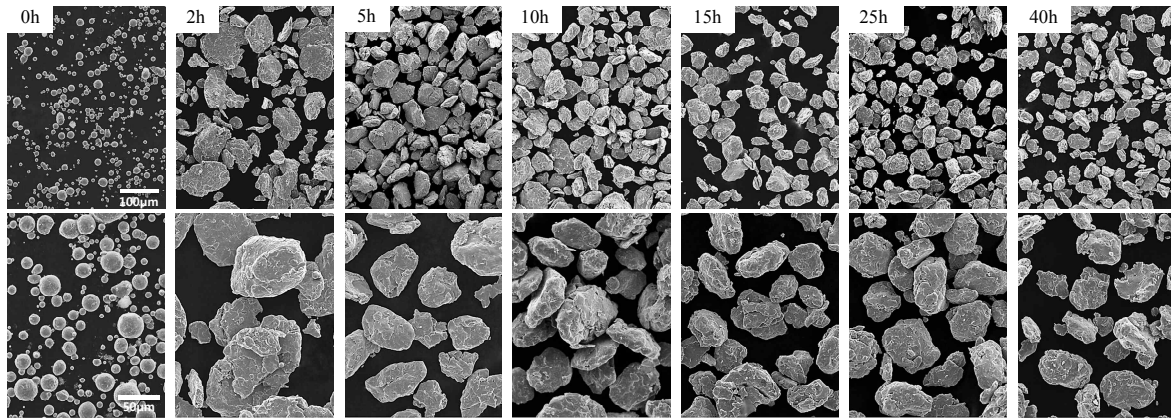


Fig. 1. Surface morphologies of mechanically alloyed powder with different length of MA time.

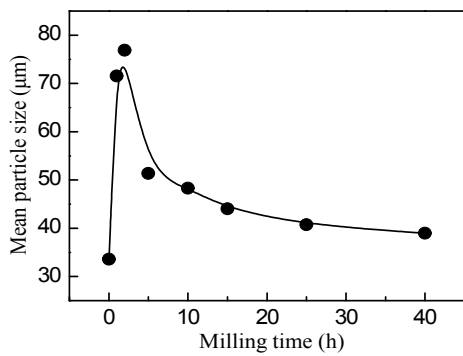


Fig. 2. Change of mean particle size with different length of MA time.

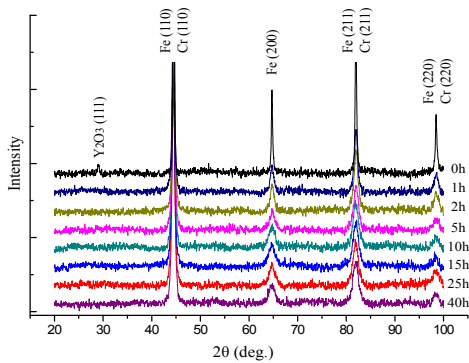


Fig. 3. XRD patterns of MA powders with different length of MA time.

The surface morphologies of mechanically alloyed powder with different length of MA times was shown in Fig. 1. Initial raw metallic powder was quite spherical shape because the powder was manufactured by high pressure Ar-gas atomization process. After 1h for the mechanical alloying process, powder showed irregularly spherical and flake shape with rough surface. As increase the milling time, a particle size was decreased with somewhat uniform flake shape. The change of mean particle size with different length of MA time was plotted in Fig. 2. The particle size was dramatically increased in the beginning stage of the MA process and this means that the cold-welding and agglomeration

phenomenon were more dominant than the pulverization by milling media. After 10h of MA, however, continuous cold-welding and pulverization occurred repeatedly because the mean particle size was decreased slightly, as milling time increased. The evolution of XRD patterns with different milling times was shown in Fig. 3. Before the MA process, a quite weak Y_2O_3 peak was identified because of a small amount of 0.35wt%, and several main diffraction peaks were also identified as bcc Fe and Cr. However an Y_2O_3 peak completely disappeared even after the mechanical alloying for 1h. This means that Y_2O_3 would be decomposed to yttrium and oxygen atoms during the MA process and dissolved in the 10Cr wt% steel matrix by repeated cold-welding and pulverization of steel balls with high impact energy [4]. The intensity of diffraction peaks decreased with increasing the mechanical alloying time. In Fig. 4, the crystallite size with different length of MA time was shown. Crystallite size of bcc iron can be estimated using the Scherrer equation:

$$D = \frac{0.9\lambda}{\beta \cos\theta}$$

where λ is X-ray wave length(=1.54Å), β is the true full width at the half maximum height(FWHM) and θ is diffraction angle. Crystallite size was sharply declined in the initial stage of MA process and finally saturated after 5h.

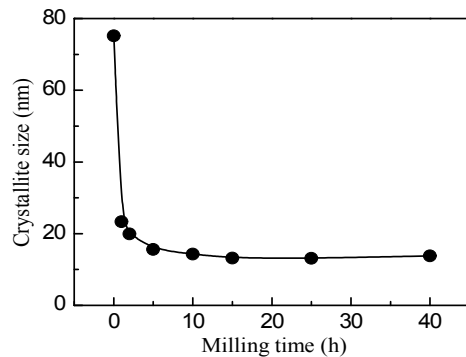


Fig. 4. Crystallite size with different length of MA time.

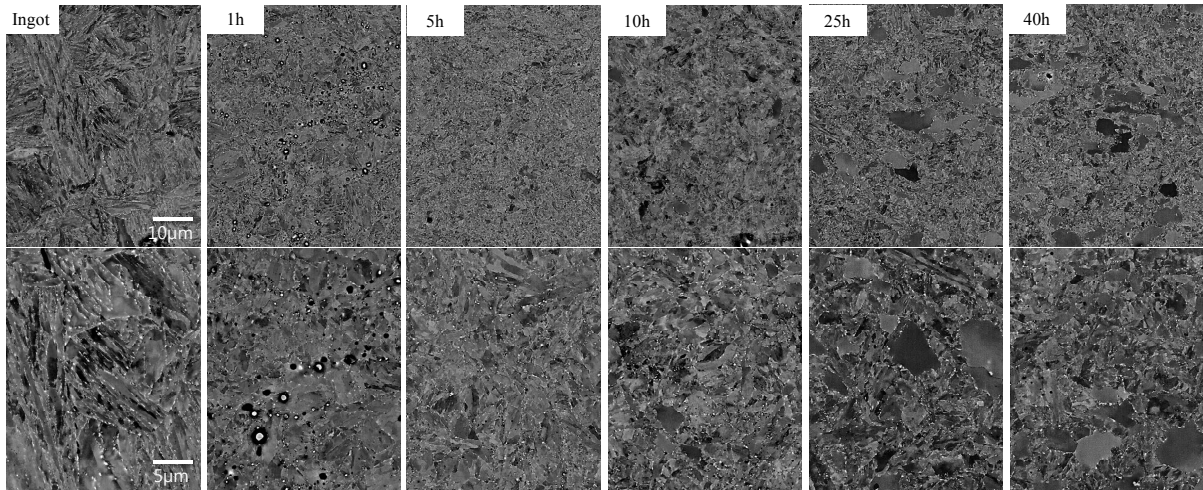


Fig. 5. SEM images of microstructures of a pre-alloyed ingot and UHP fabricated ODS steels with different length of mechanical alloying time.

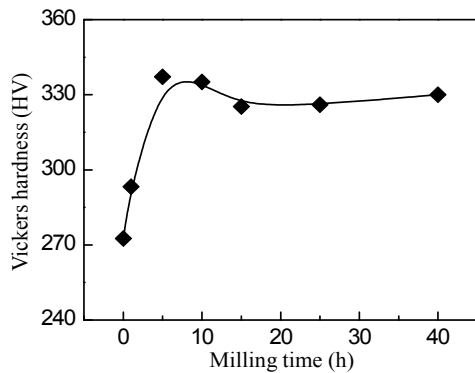


Fig. 6. Hardness change of UHPed ODS steels with different milling time.

2.3 Microstructure evolution of consolidated ODS steels with different length of MA time

ODS steels can be fabricated by various consolidation processes such as hot isostatic pressing and hot extrusion. In this study, uniaxial hot pressing (UHP) was employed to fabricate the ODS steel samples easily. The SEM images of microstructures of a pre-alloyed ingot and UHP fabricated ODS steels were shown in Fig. 5. Microstructure of a pre-alloyed ingot shows a typical tempered martensite with prior austenite grains and fine lath structures. This is a representative microstructure which is shown in high Cr heat-resistant ferritic/martensitic steels. They usually have carbides, $M_{23}C_6$ ($M=Cr, Fe, W, Mo$) in several tens of nm on the grain boundaries. The carbide distribution was observed as white dots, because of back-scattered electron images by a FE-SEM. After 1h MA, inhomogeneous grain morphology was observed as well as coarse carbides distribution. Black dots were also co-existed which are oxides such as Y_2O_3 and TiO_2 . This means that sufficient mechanical alloying is not carried out, so that precipitate phases are temporarily located between powder and powder, this resulted that inhomogeneous

grains and coarse precipitates are distributed. Quite homogenous distribution of fine grains and precipitates was observed after 5-10h MA. In the longer length of MA time, after 25-40h, abnormal growth grains were partially observed and this is assumed that impurities from milling medium materials and oxygen are penetrated due to repeated milling operation. Hardness change of UHPed ODS steels with different length of MA time is plotted in Fig. 6. Coincided with microstructures, ODS steel milled 5h had the highest hardness. Further analysis is needed for nano-oxide particle distributions, however, milling of 5-10h is sufficient for homogeneous grain structure.

3. Conclusions

In this study, powder properties and microstructures of the ODS steel with different length of mechanical alloying time was investigated. The ODS steel milled 5h showed homogeneous grain structure with the highest hardness.

Acknowledgements

This work was supported by the National Research Foundation of Korea(NRF) grant funded by the Korea government(MEST) (NRF-No. 2012M2A8A1027872).

REFERENCES

- [1] T.K. Kim, S.H. Kim, Journal of Nuclear Materials, Vol. 411, pp. 208, 2011.
- [2] T. Lechtenberg, Journal of Nuclear Materials. Vol. 133, pp. 149, 1985.
- [3] B. Raj, M. Vijayalakshmi, Comprehensive of Nuclear Materials, p. 97-121, Elsevier, Holland, 2012.
- [4] T. Okuda, M. Fujiwara, Journal of Materials Science Letters, Vol. 14, pp. 1600-1603, 1995.